Electronic Supplementary Material (ESI) for Dalton Transactions.

Supporting Information

Novel core-shell-like nanocomposites *x*Cu@Cu_2O/MgAlO-rGO through *in situ* self-reduction strategy for highly efficient reduction of 4-nitrophenol

Liguang Dou, Yanna Wang, Yangguang Li and Hui Zhang*

State Key Laboratory of Chemical Resource Engineering, Beijing University of Chemical Technology, Beijing 100029, China.

*Correspondence should be addressed to Hui Zhang.
E-mail: Huizhang67@gst21.com
Tel.: +8610 64425872
Fax: +8610 64425385

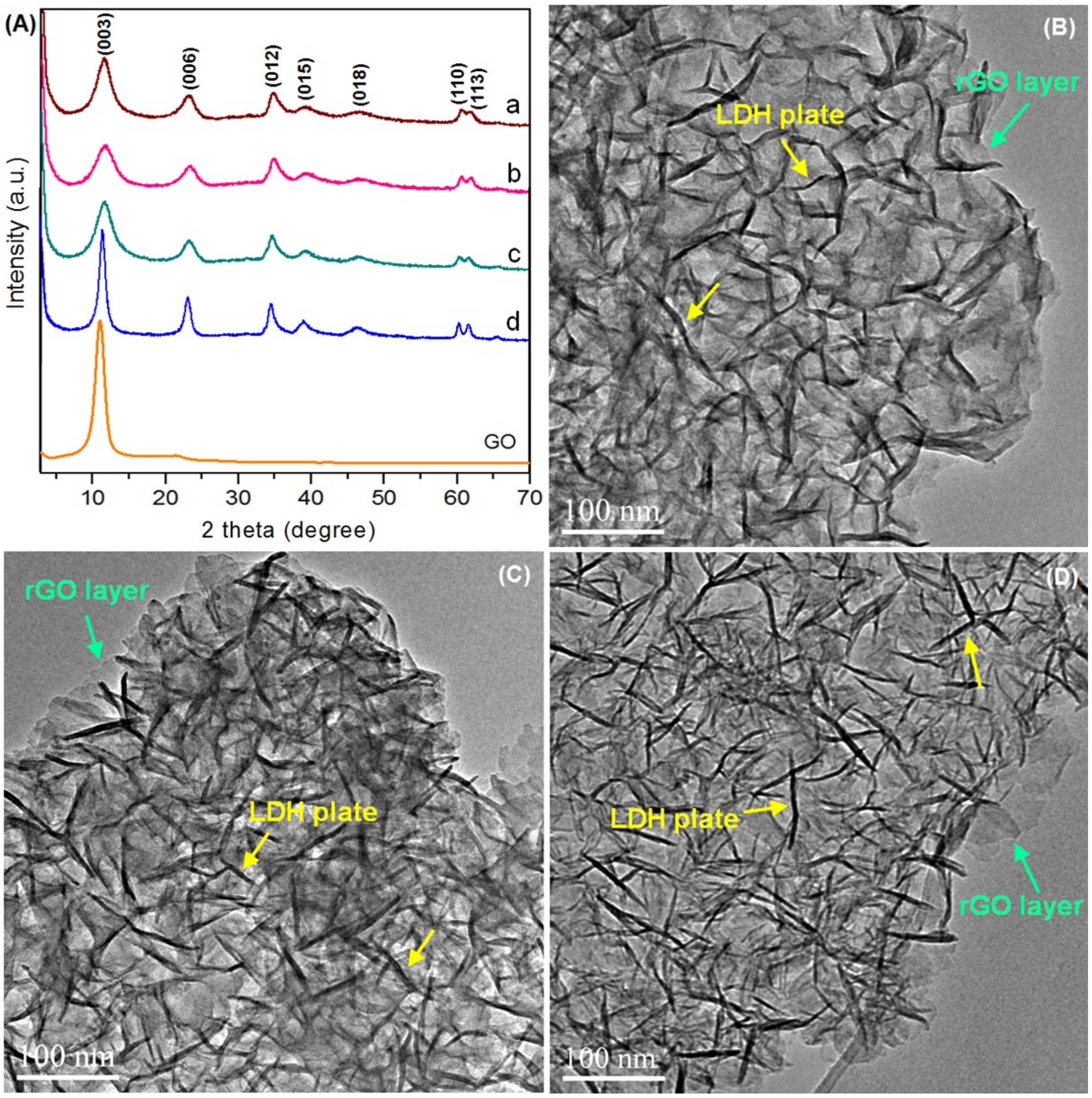

Figure S1. (A) XRD patterns of the as-prepared hybrid precursors $Cu_{0.5}Mg_{2.5}Al$-LDH/rGO (a), Cu_1Mg_2Al-LDH/rGO (b), $Cu_{1.5}Mg_{1.5}Al$-LDH/rGO (c) pure CuMgAl-LDH (d) and GO. (B-D) TEM images of $Cu_{0.5}Mg_{2.5}Al$-LDH/rGO (B), Cu_1Mg_2Al-LDH/rGO (C) and $Cu_{1.5}Mg_{1.5}Al$-LDH/rGO (D).

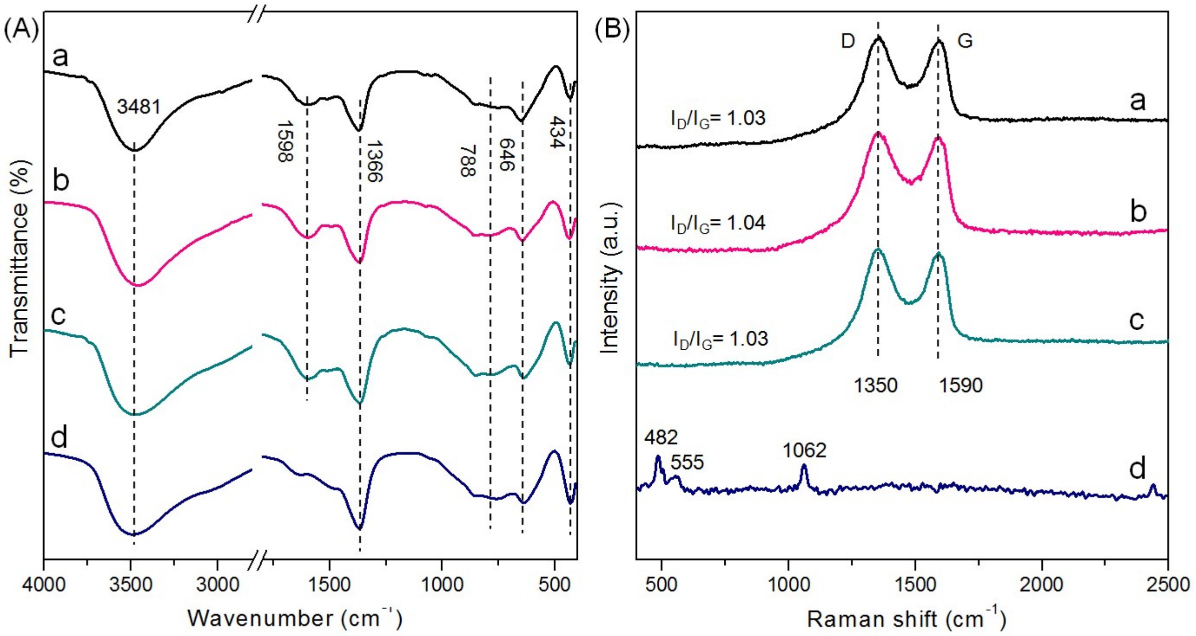

Figure S2. (A) FTIR and (B) Raman spectra of the precursors $Cu_{0.5}Mg_{2.5}$Al-LDH/rGO (a), Cu_1Mg_2Al-LDH/rGO (b), $Cu_{1.5}Mg_{1.5}$Al-LDH/rGO (c) and CuMgAl-LDH (d).

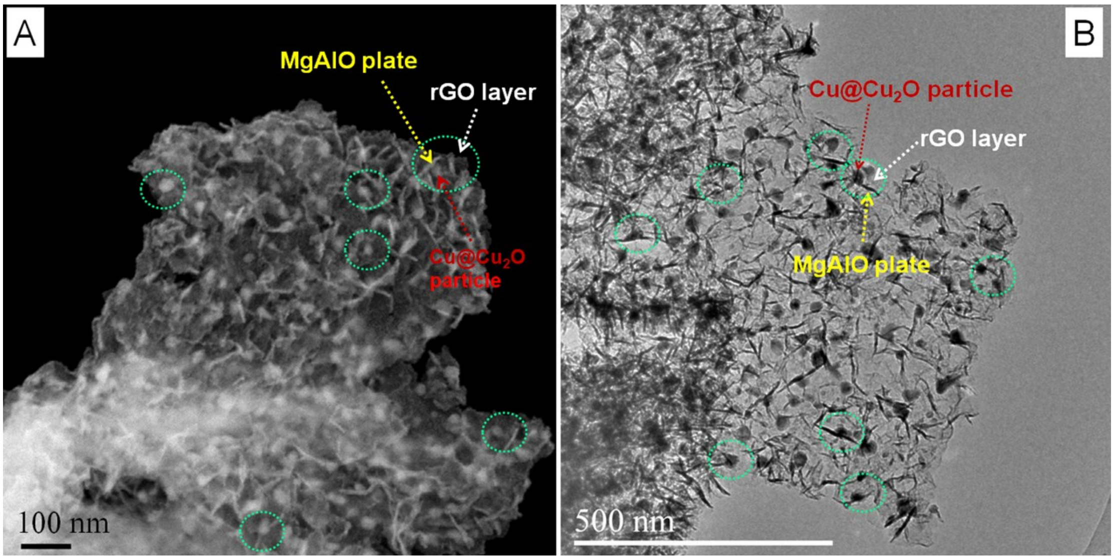

Figure S3. Low-magnification (A) SEM and (B) TEM images of typical 1.0Cu@Cu_2O/MgAlO-rGO.

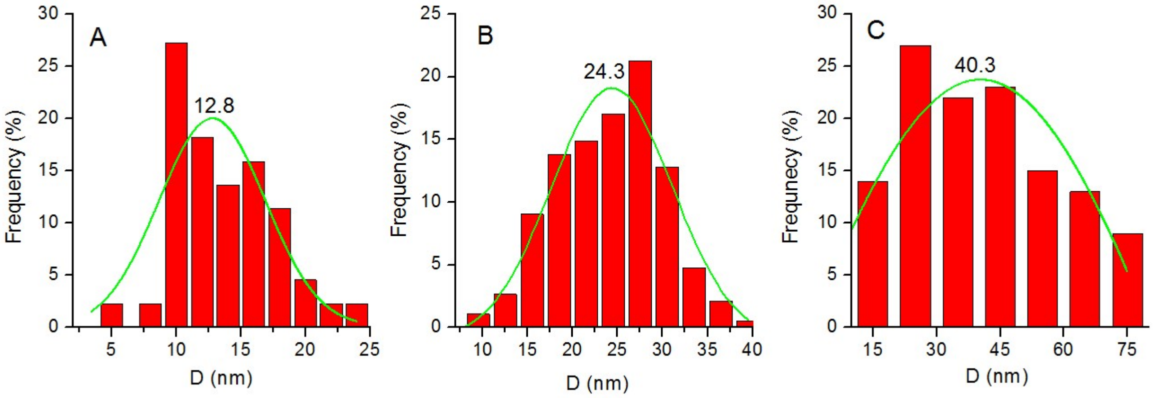

Figure S4. The particle size distribution of 0.5Cu@Cu_2O/MgAlO-rGO (A), 1.0Cu@Cu_2O/MgAlO-rGO (B) and 1.5Cu@Cu_2O/MgAlO-rGO (C).

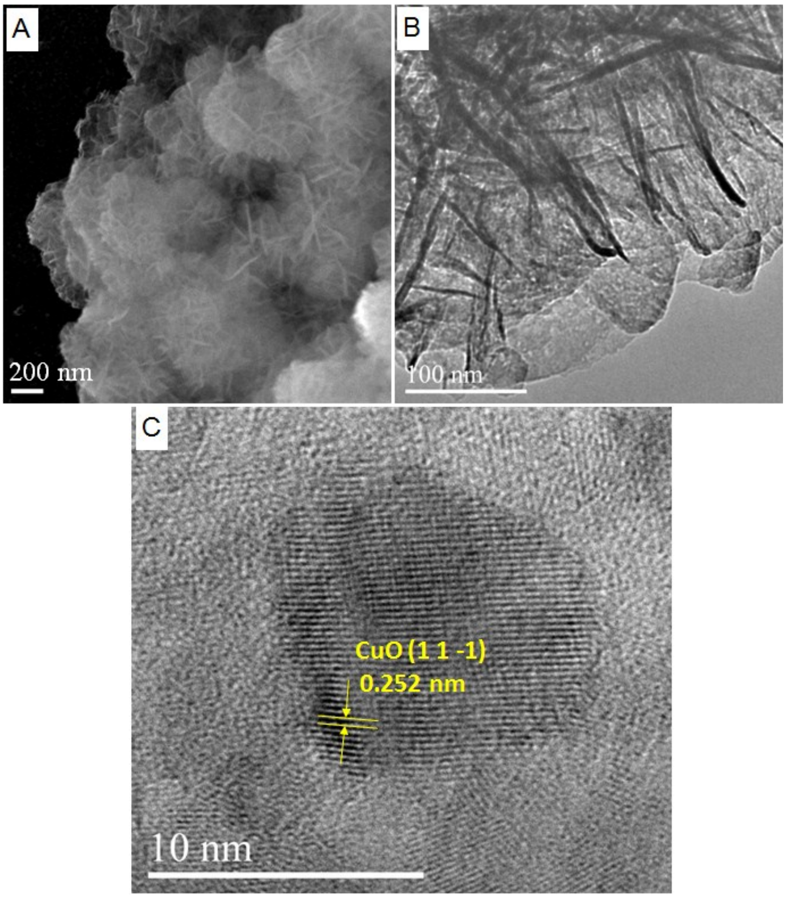

Figure S5. The (A) SEM, (B) TEM and (C) HRTEM images of 1.0CuMgAlO.

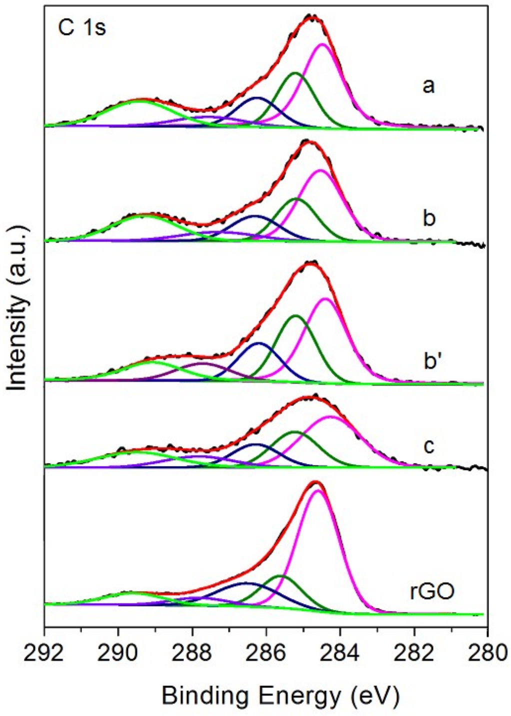

Samples	B. E. (eV)	
	C=C	C-C
0.5Cu@Cu_2O/MgAlO-rGO	284.49	285.21
1.0Cu@Cu_2O/MgAlO-rGO	284.54	285.19
Cu_1Mg_2Al-LDH/rGO	284.40	285.20
1.5Cu@Cu_2O/MgAlO-rGO	284.26	285.23
rGO	284.59	285.60

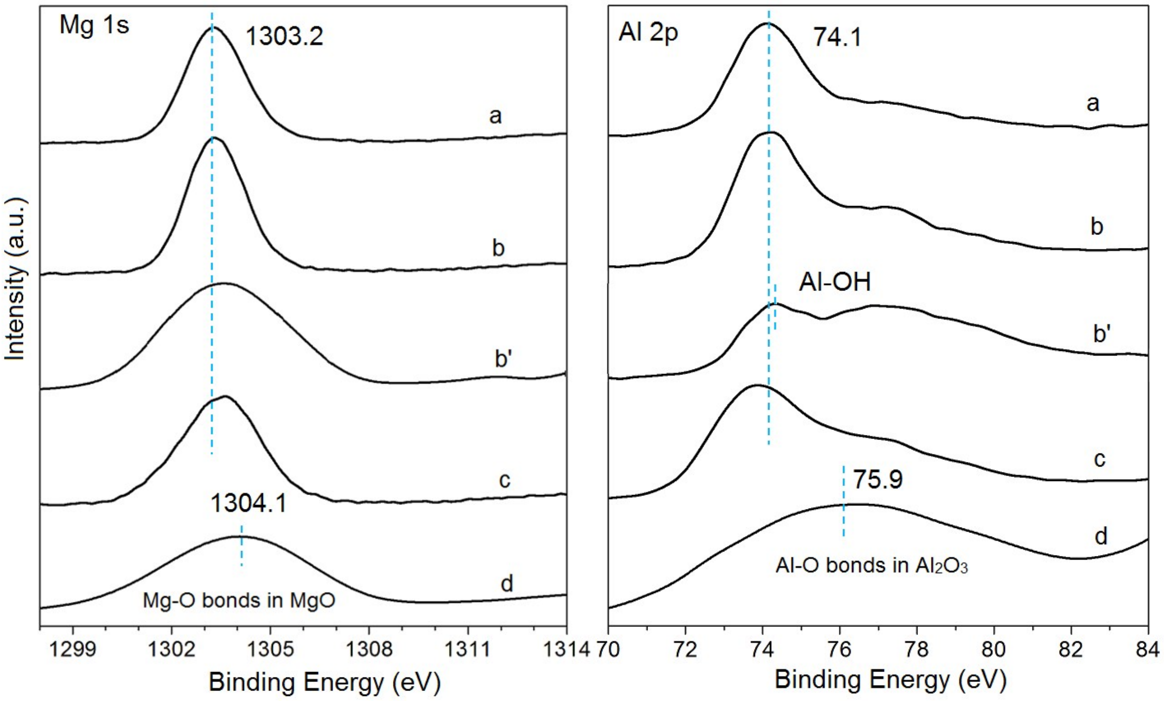

Figure S6. C 1s, Mg 1s, and Al 2p XPS spectra of 0.5Cu@Cu_2O/MgAlO-rGO (a), 1.0Cu@Cu_2O/MgAlO-rGO (b), Cu_1Mg_2Al-LDH/rGO (b'), 1.5Cu@Cu_2O/MgAlO-rGO (c), 1.0CuMgAlO (d) and rGO.

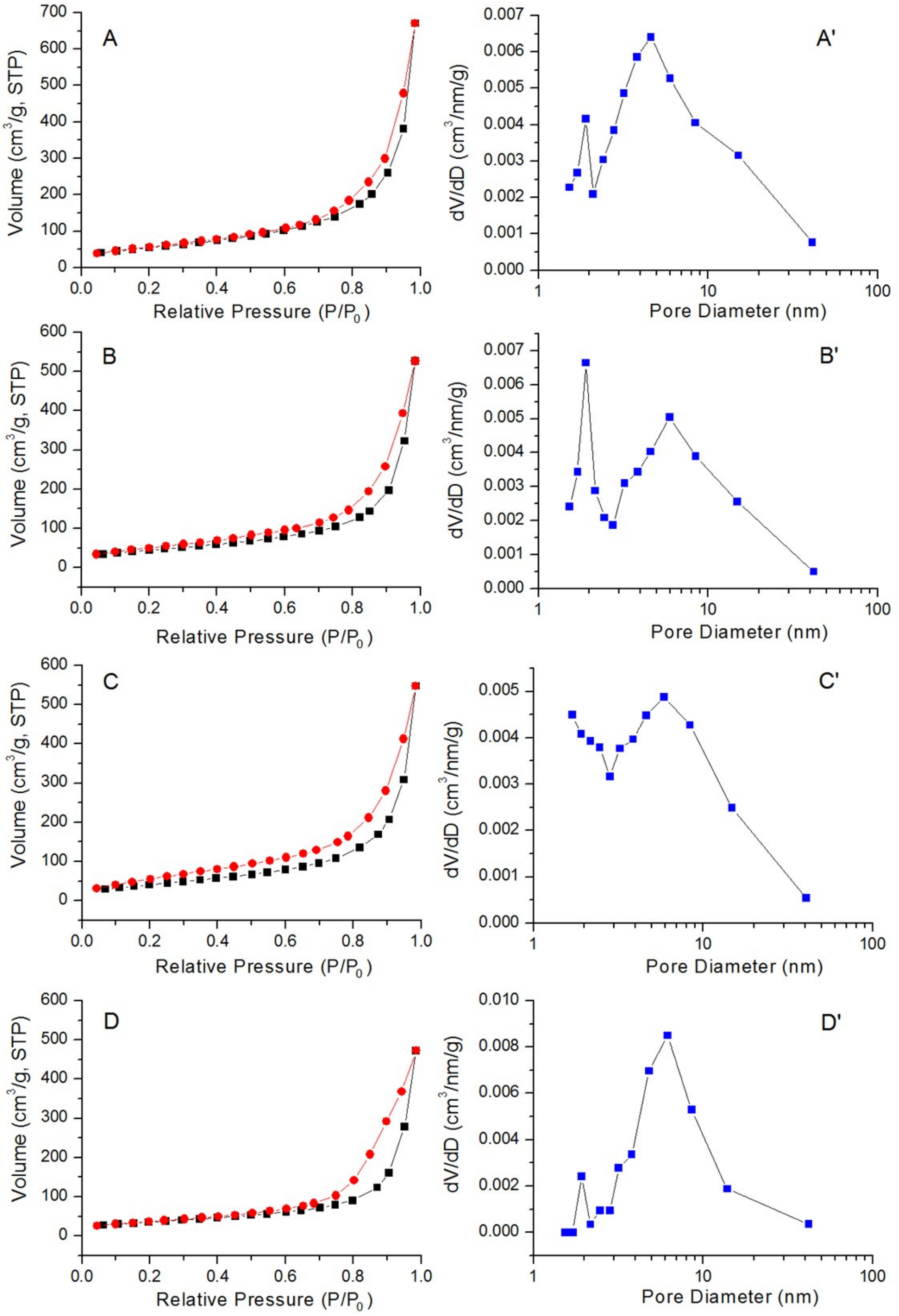

Figure S7. Low temperature N_2 adsorption-desorption isotherms (A-D) and BJH pore size distributions (A'-D') of 0.5Cu@Cu_2O/MgAlO-rGO (A, A'), 1.0Cu@Cu_2O/MgAlO-rGO (B, B'), 1.5Cu@Cu_2O/MgAlO-rGO (C, C') and 1.0CuMgAlO (D, D').

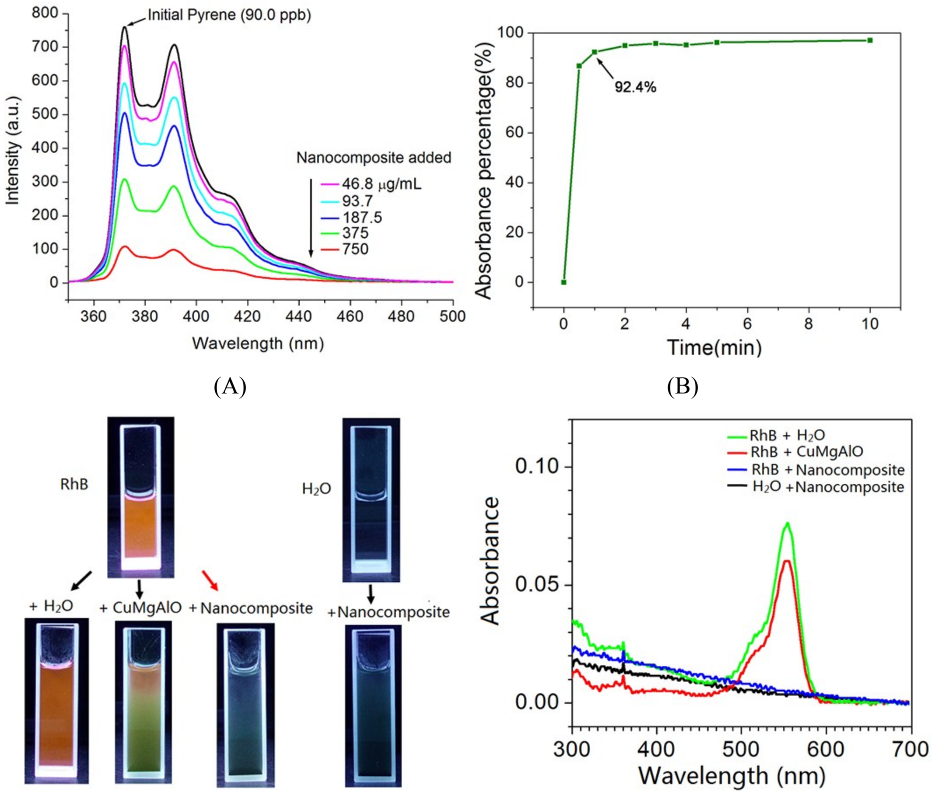

(A) (B)

(C) (D)

Figure S8. Evidence of *π*-*π* stacking: (A) fluorescence quenching of pyrene-contaminated water by adding 1.0Cu@Cu_2O/MgAlO-rGO suspensions with varied concentrations (46.8-750 μg/mL). Conditions: λ_{ex} = 335 nm; initial concentration of pyrene = 90.0 ppb; adsorption time: 1.0 min. (B) Time-dependent adsorption percentage of pyrene by 1.0Cu@Cu_2O/MgAlO-rGO on fluorescence analyses (nanocomposite: 750 μg/mL). (C) Digital photo of RhB solution with the hybrid 1.0Cu@Cu_2O/MgAlO-rGO and 1.0CuMgAlO under UV light (365 nm). Conditions: RhB, 836 ppb (2 mL); catalyst, 2.5 mg/mL (1 mL). (D) UV-vis spectra of the centrifuged supernatants in (C)

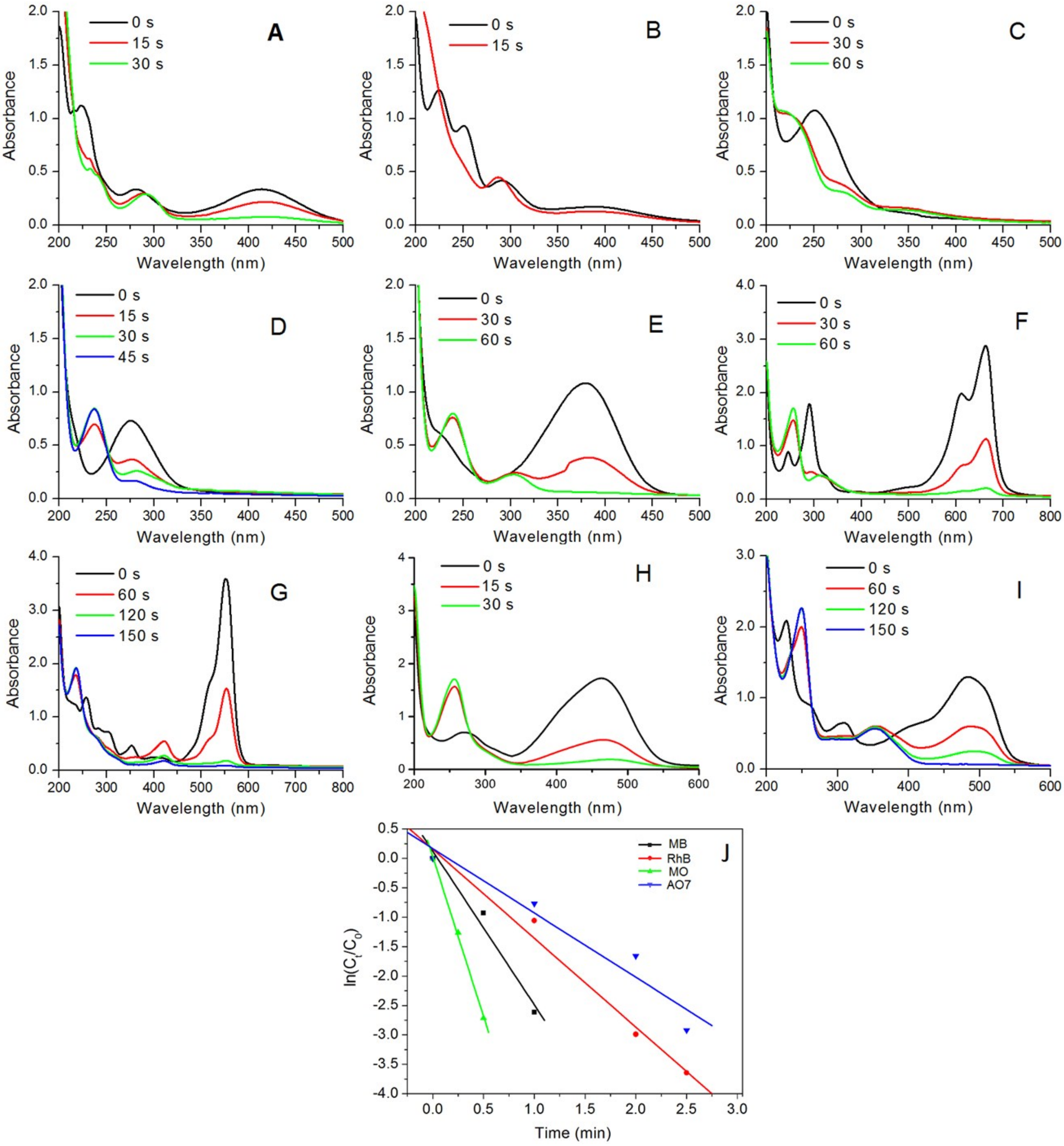

Figure S9. UV-vis absorption spectra of the reduction and degradation of diverse nitroarenes (A: 2-NP, B: 3-NP, C: 2,4-dinitrotoluene, D: 4-nitrobenzaldehyde, and E: 4-nitroaniline) and organic dyes (F: MB, G: RhB, H: MO and I: AO7) by $NaBH_4$ with the catalyst $1.0Cu@Cu_2O/MgAlO$-rGO, and plots of $\ln(C_t/C_0)$ versus time for the reduction of MB, RhB, MO and AO7 over $1.0Cu@Cu_2O/MgAlO$-rGO.

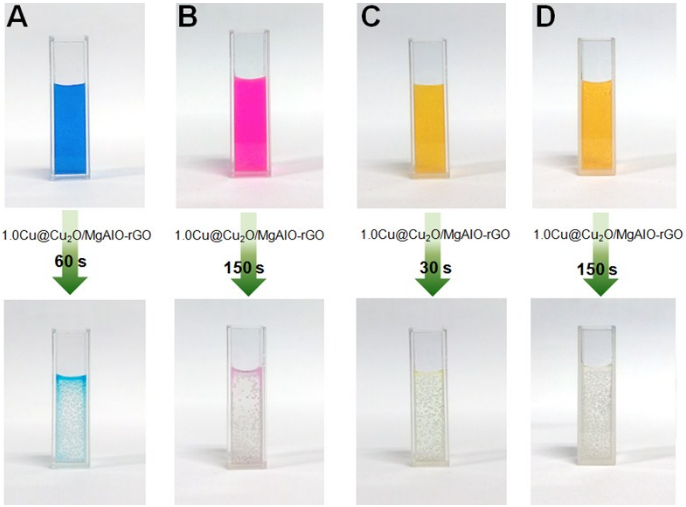

Figure S10. The color change of the MB (A), RhB (B), MO (C) and AO7 (D) when catalyzed by the 1.0Cu@Cu_2O/MgAlO-rGO in the presence of $NaBH_4$.

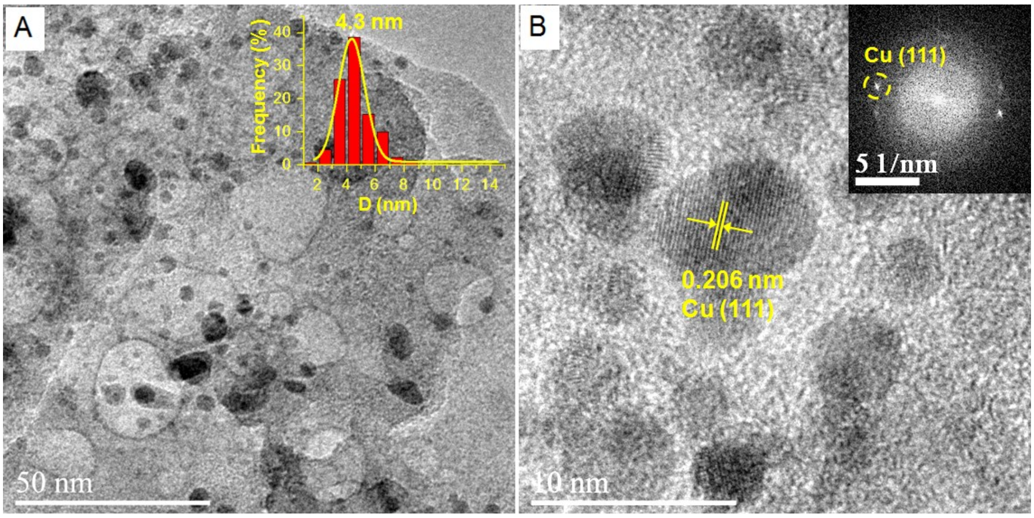

Figure S11. (A) TEM and (B) HRTEM images of 1.0Cu@Cu_2O/MgAlO-rGO recovered from the 25th cycle of the catalytic reduction of 4-NP (inset in A, the particle size distribution on more than 300 particles; inset in B, the corresponding FFT pattern).

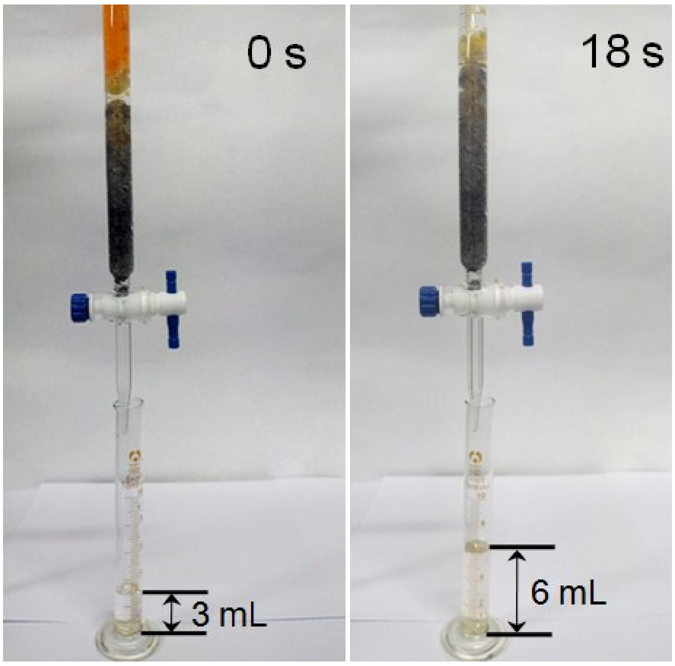

Figure S12. Photographs showing the setup and the complete reduction of 3 mL of the mixture of 4-NP (1 mM) and MO (1 mM) in 18 s by 1.0Cu@Cu_2O/MgAlO-rGO. The total Cu in the column is 6.68 mg.

Table S1. Chemical composition and structural data for *x*Cu@Cu_2O/MgAlO-rGO and 1.0CuMgAlO.

Samples	Bulk Cu /wt% [a]	Surface Cu /wt% [b]	D_{111}/nm (Cu) [c]	D_{200}/nm (Cu) [c]	D_{111}/nm (Cu_2O) [d]	S_{BET} /m^2g^{-1} [e]
0.5Cu@Cu_2O/MgAlO-rGO	10.76	5.23	8.5	-	10.2	199.3
1.0Cu@Cu_2O/MgAlO-rGO	19.09	7.42	12.5	13.4	12.9	159.8
1.5Cu@Cu_2O/MgAlO-rGO	27.70	9.43	17.4	16.4	18.2	157.6
1.0CuMgAlO	21.30	15.50	-	-	-	125.2

[a] Determined by ICP analysis. [b] Determined by XPS analysis. [c] Based on XRD line broadening of (111) plane at 43.3° and (200) plane at 50.4° for cubic Cu. [d] Based on XRD line broadening of (111) plane at 36.4° for cubic Cu_2O. [e] BET surface area.

Table S2. Catalyzing reduction and degradation of diverse nitroarenes and organic dyes over 1.0Cu@Cu_2O/MgAlO-rGO.

Entry	Substrate	Time (min)[a]	TOF (h^{-1})
1	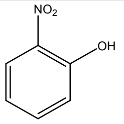	0.5	399.2
2	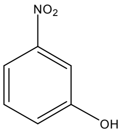	0.25	798.3
3	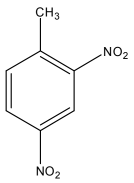	1.0	199.6
4	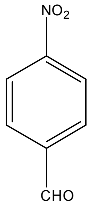	0.75	266.1

5	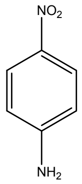	1.0	199.6
6	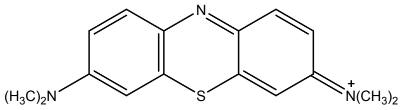	1.0	199.6
7	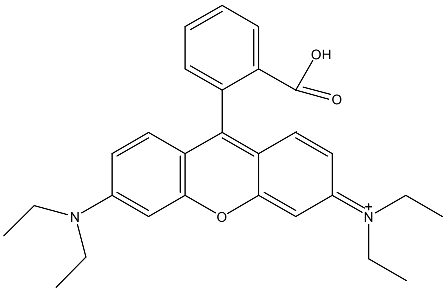	1.5	133.0
8	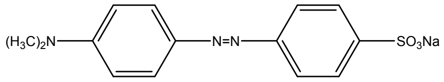	0.5	399.2
9	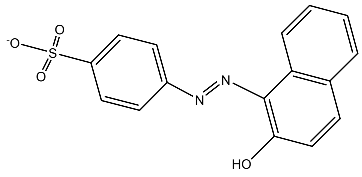	1.5	149.7